

Piotr P. Goldstein¹ ORCID 0000-0002-0236-5332

Some exact results on the Belinski-Khalatnikov-Lifshitz scenario

*1

¹*Theoretical Physics Division National Centre for
Nuclear Research, Pasteura 7, Warsaw, Poland*

(Dated: June 5, 2025)

arXiv:2505.15541v1 [gr-qc] 21 May 2025

¹ email: piotr.goldstein@ncbj.gov.pl

Abstract

The well-known Belinski-Khalatnikov-Lifshitz (BKL) scenario for the universe near the cosmological singularity is supplemented with a few exact results following from the BKL asymptotic of the Einstein equations: (1) The cosmological singularity is proved to be an inevitable beginning or end of the universe as described by these equations. (2) Attaining the singularity from shrinking initial conditions requires infinite time parameter τ ; no singularity of any kind may occur in a finite τ . (3) The previously found exact solution [P.G. and W. Piechocki, Eur. Phys. J. C 82:216 (2022)] is the only asymptotic with well-defined proportions between the directional scale factors which have been appropriately compensated against indefinite growth of anisotropy. In all other cases, the universe undergoes oscillations of Kasner type, which reduce the length scales to nearly zero in some directions, while largely extending it in the others. Together with instability of the exact solution [op. cit.], it makes the approach to the singularity inevitably chaotic. (4) Reduced equations are proposed and explicitly solved to describe these oscillations near their turning points. In logarithmic variables, the oscillations are found to have sawtooth shapes. A by-product is a quadric of kinetic energy, a simple geometric tool for all this analysis.

CONTENTS

I. Introduction	3
II. Basic properties of the BKL equations	6
III. Methods	7
A. Useful variables	7
B. The cone of kinetic energy	9
IV. Solutions ending at the apex of the cone	12
A. The exact solution in the cone	12
B. On the uniqueness of the exact solution	13
V. Solutions approaching the lateral surface of the cone	13
A. Asymptotics of the diagonal velocities	14
B. Impossibility of the exact Kasner asymptotics	14
VI. Quasi-Kasner solutions	15
A. Description	15
B. Between Kasner's epochs	16
VII. Conclusions	20
A. Proof that asymptotic of the exact solution is the only path to the collapse with well-defined proportions between q , r , s (Proposition 9)	20
B. Proof that all trajectories eventually tend to the apex (Proposition 10)	21
References	22

I. INTRODUCTION

The Belinski-Khalatnikov-Lifshitz (BKL) scenario plays a significant role among classical descriptions of the universe close to the cosmological singularity. It has been developed as an answer to the question whether the singularity follows from the Einstein equations for a set of nonzero measure on the manifold of initial or final conditions [1]. The manifold should have the proper dimensionality, i.e., depend on the proper number of arbitrary parameters. Moreover, the singularity should be physical reality rather than a result of simplifying assumptions of a simplistic model or a choice of a special frame of reference.

The first question concerned the sheer existence of such a singularity. The initial approach in [1] gave the negative answer to this question. Namely, the authors demonstrated possibility of transformation to the synchronous frame of reference (in which time is the proper time at each point) and proved that all solutions having the required properties, such that the corresponding determinant of the spatial metric tensor vanishes in a finite time, are fictitious because the singularity may vanish in other reference systems. However, later R. Penrose [2] and S. Hawking [3] proved existence of a singularity independent of the frame of reference, first for the case of a collapsing star [2], then for a class of cosmological models [3]. This made the authors of [1] reconsider their assertion. To obtain a universe with a physical singularity, BKL considered [4] possible generalizations of Kasner's homogeneous universe without matter [5].

The original Kasner's solutions exactly satisfy the Einstein equations without the energy-momentum term. They describe an Euclidean metric; for orthogonal principal directions, it reads [5]

$$ds^2 = dt^2 - (t^{2p_1} dx_1^2 + t^{2p_2} dx_2^2 + t^{2p_3} dx_3^2) \quad (1)$$

where the constants p_1, p_2, p_3 satisfy

$$p_1 + p_2 + p_3 = 1 \quad \text{and} \quad p_1^2 + p_2^2 + p_3^2 = 1. \quad (2)$$

As (2) infers that one of these exponents has to be negative, the Kasner solutions are singular at $t = 0$. Moreover, they are anisotropic, and their anisotropy, measured by ratios of scales in the principal spatial directions, grows indefinitely on the approach to the singularity (with the exception of $p_1 = p_2 = 0, p_3 = 1$, up to exchange of the indices). The differential of the volume is proportional to t , hence its limit is equal to 0 if $t \rightarrow 0^+$.

The Kasner metric (1) may be one of the possible answers to another important question: on symmetries of the primordial universe, close to the singularity. Although the recent universe is isotropic, it does not mean that it has been isotropic from the beginning. Therefore, cosmological models allowing for primordial anisotropy should be taken into consideration.

The authors of [4] looked for a generalization of the Kasner solutions to a possibly large class preserving Kasner's properties: homogeneity and increasing anisotropy on the approach to the singularity. The asymptotic behavior of the universe under these assumptions is known as the BKL scenario. Limiting the interest to the region close to the singularity allows for reduction of the Einstein equations to relatively simple ordinary differential equations (ODE).

For completeness, we provide a short summary how these ODE follow from their Einstein origin, as derived in [6].

(i) In the neighborhood of the singularity, the influence of matter, described by the r.h.s. of the Einstein equations, i.e., the energy-momentum tensor, may be neglected. This assumption is based on the observation [4] that the energy-momentum term has higher order

in time (if the singularity is at $t = 0$), compared to the singular behavior of the spacetime curvature. (ii) For further calculations, the authors of [4] choose the synchronous frame of reference. This choice allows for assuming the metric tensor in the form

$$ds^2 = dt^2 - \gamma_{ab}(t)dx^a dx^b, \quad (3)$$

where γ_{ab} are components of the spatial metric tensor in the coordinate system x^a , $a = 1, 2, 3$ (summation convention is used to covariant-contravariant pairs of indices).

Metric (3), substituted to the Einstein equations, reduces the 4-dimensional (4D) problem to a problem of finding a 3D metric. In the Bianchi classification, the corresponding Lie algebra is Bianchi IX. (iii) Its structure constants are chosen as ε_{abc} , where ε is the Levi-Civita antisymmetric symbol.

(iv) For the sake of simplicity, dt in (3) is rescaled by the factor of the spatial volume, according to

$$dt = \sqrt{\gamma} d\tau, \quad (4)$$

where γ is the determinant of the spatial (time-dependent) metric tensor γ_{ab} ($a, b = 1, 2, 3$). In Kasner's metric, we have $\sqrt{\gamma} = t$, whence τ is a logarithmic time parameter, $d\tau = d \ln t$. This way, the singularity at $t = 0$ appears as the limit $\tau \rightarrow -\infty$ or (by symmetry of the resulting equations) $\tau \rightarrow \infty$. The latter is our choice of this time parameter. With this choice, a collapse at $\tau \rightarrow \infty$ will correspond to $t \rightarrow 0^+$ i.e. to the backward trip down to the initial singularity.

(v) Of the ten Einstein equations for the spacetime without matter, those describing the time-spatial, i.e. 0_a components, are found to provide only relations between constants; they do not describe the dynamics. What remains are 3 diagonal and 3 off-diagonal equations for the spatial, i.e. b_a components, and one equation for the temporal 0_0 component. (vi) The order 2 of the off-diagonal spatial equations is reduced to 1 with the aid of the Bianchi identities. (vii) Two of three corresponding constants of the integration are set to 0, which determines the orientation of the chosen coordinate system (thus further specifying the frame of reference).

(viii) In general, the principal axes of the spatial metric tensor would rotate with respect to the chosen fixed frame. However, it is proven that the rate of the rotation (e.g. in terms of the Euler angles) tends to zero on the approach to the singularity, provided that the ratios of the two shorter length scales along the principal axes to the longest one tend to zero (this is the indefinitely growing anisotropy). Hence, the angles tend to the respective constant values on the approach to the singularity. This reduces the task to solving one temporal ODE and three spatial ODE for these length scales.

(ix) In the zero order in the aforementioned ratios of scales, we obtain the required three spatial ODE, namely

$$\frac{d^2 \ln a}{d\tau^2} = \frac{b}{a} - a^2, \quad \frac{d^2 \ln b}{d\tau^2} = a^2 - \frac{b}{a} + \frac{c}{b}, \quad \frac{d^2 \ln c}{d\tau^2} = a^2 - \frac{c}{b}. \quad (5)$$

where quantities $a = a(\tau)$, $b = b(\tau)$ and $c = c(\tau)$ are, up to constants of order 1, proportional to squares of the length scales in three principal directions of the chosen synchronous reference system. They are known as directional scale factors. The anisotropy assumption results in $a \gg b \gg c$.

These ODE are subject to the constraint imposed by the temporal equation

$$\frac{d \ln a}{d\tau} \frac{d \ln b}{d\tau} + \frac{d \ln a}{d\tau} \frac{d \ln c}{d\tau} + \frac{d \ln b}{d\tau} \frac{d \ln c}{d\tau} = a^2 + \frac{b}{a} + \frac{c}{b}, \quad (6)$$

Equations (5), together with (6), will be shortly called the BKL equations. Due to their time-reversibility, they may describe both, expansion of the universe starting from the singularity or its final collapse.

Numerous papers, were devoted to both analytic and numeric analyses of the BKL scenario, e.g. [4, 6–8]. A Hamiltonian approach was analyzed in detail in [9], and a comparison with the diagonal Mixmaster universe was done in [10]. The scenario was discussed in detail, on a broad background of related Bianchi models, in the book by Belinski and Henneaux [11].

The goal of the present paper is to supplement their work by a few exact results. All of them may be attained within the physics described by the BKL equations (5), (6). The first result was obtained in our previous paper with W. Piechocki [12], where we found an exact solution of these equations. Namely, the solution reads

$$a(\tau) = \frac{3}{|\tau - \tau_0|}, \quad b(\tau) = \frac{30}{|\tau - \tau_0|^3}, \quad c(\tau) = \frac{120}{|\tau - \tau_0|^5} \quad (7)$$

where $|\tau - \tau_0| \neq 0$ and τ_0 is an arbitrary real number.

In [12], we also found that the exact solution (7) is unstable to small perturbations of the initial conditions. In more detail, the perturbations evolve into two oscillatory components. Although their amplitudes tend to zero as $\tau \rightarrow \infty$, the instability is manifested in the growth of the ratios of the perturbation amplitudes to the respective perturbed scale factors; these ratios increase as $\tau^{1/2}$. A characteristic value of the ratio between the two oscillation frequencies (approximately equal to 2.06) is one of the results of [12]; some chance exists that this ratio could have left marks in the spectra of presently observed waves.

The new exact results which are demonstrated in this paper are

1. All solutions of the BKL equations in which the initial volume decreases with the time parameter τ , i.e. $dV/d\tau|_{\tau=0} < 0$, lead to the total collapse (in all three directions) for $\tau \rightarrow \infty$ (subsection V B, Proposition 10).
2. For such initial conditions, no singularity occurs in finite τ , i.e., the scale factors remain finite and nonzero (subsection III B, Proposition 7).
3. The exact solution is the only one which collapses with well-defined proportion between ratios of the directional scale factors raised to the appropriate powers (the raising to power compensates for the indefinitely growing anisotropy). For all other solutions of (5), (6), the collapse is attained through infinitely many oscillations between Kasner's epochs (such behavior was already found in a different approach to the asymptotics in [13] and in [4]). If we approach the singularity for $t \rightarrow 0^+$, the frequency of the oscillations must tend to infinity and thus the approach is chaotic. Together with the previously found [12] instability of this only exception, it infers that chaos on the approach to the singularity is inevitable (subsection IV B, Proposition 9).
4. BKL have shown that the dynamics is indeed Kasner-type and each solution of this type loses its validity after some time [6]. Then the role of the p_i , $i = 1, 2, 3$ in equations (1) and (2) is exchanged, i.e. transition to another Kasner epoch occurs [6] (like in the Mixmaster universe [5]). This is the oscillatory approach to the singular point, predicted in [4]. In the present paper, we provide explicit description of the dynamics in the transition period between the epochs (subsection VI B). It results

(among other things) in finding that these are sawtooth oscillations in the logarithmic variables, with explicitly calculable gradients of the teeth.

A by-product of the calculation is a cone (more general – a quadric) of kinetic energy, a simple geometric tool whose role is similar to the well-known diagrams invented by Misner [5]; it is described in detail in subsection III B.

This paper is structured as follows:

In section II, the basic information on the BKL scenario is shortly summarized. It includes the basic properties of equations (5), (6) and their Lagrangian-Hamiltonian structure. Section III contains description of methods, especially the geometric tool of the present analysis, which is the cone of the kinetic part of the Lagrangian (further called “kinetic energy”). Section IV contains (in IV B) one of the main results, which is uniqueness of the exact solution (7) as the only one in which the collapse of the universe has a definite proportion of the length scales (raised to the appropriate powers to compensate for the indefinitely growing anisotropy). In section V, the Kasner-type solutions are described. A result stating that the BKL equations are not satisfied by the exact Kasner solutions, even in the limit $\tau \rightarrow \infty$, is given in subsection V B. Section VI is devoted to the Kasner-type solutions, with subsection VI B discussing details of the transitions between the adjacent Kasner epochs.

Most results are organized in a system of simple propositions and their straightforward proofs. The proofs longer than a few lines have been put off to two appendices.

II. BASIC PROPERTIES OF THE BKL EQUATIONS

Symmetries: [15] The way in which equations, (5), (6) were obtained determines that there is no symmetry under permutation of a , b and c . On the contrary, the growing anisotropy assumption results in $a \gg b \gg c$. The system is evidently symmetric under time reversal $\tau \rightleftharpoons -\tau$; thus it can describe the universe in both, a collapse or an explosion as its reversal. The equations have two Lie symmetries [15]. The first one is a shift in the time parameter $\tau \rightleftharpoons \tau - \tau_0$ for any τ_0 (which is obvious for an autonomous system). The second is a scaling symmetry: If a , b and c constitute a solution of (5), (6), and λ is the scaling parameter, such that

$$\tau' = \lambda\tau, \quad a' = a/\lambda, \quad b' = b/\lambda^3, \quad c' = c/\lambda^5, \quad (8)$$

then a' , b' and c' as functions of τ' make another solution of the system [15].

Dependence: At first glance, system (5), (6) appears to be overdetermined, due to the constraint (6) imposed on solutions of (5). However, the constraint (6) specifies a value of a first integral of (5). Therefore, each of the equations (5) may be obtained from a system consisting of the other two of (5) and the constraint (6). E.g. [15], if we substitute \ddot{a} and \ddot{b} from the first two of the equations (5) into the τ -derivative of the constraint (6), we obtain the third equation of (5) multiplied by $(\dot{a}/a + \dot{b}/b)$ (the dot denotes τ differentiation). This way, the third equation of (5) is shown to be dependent on the other two and the constraint (6) (the expression in the parentheses yields $ab = \text{const.}$, which is inconsistent with equations (5), (6)).

Canonical structure [9] Substitution

$$a = \exp(x_1), \quad b = \exp(x_2), \quad c = \exp(x_3) \quad (9)$$

yields a system derivable from a Lagrangian

$$\mathcal{L} = \dot{x}_1\dot{x}_2 + \dot{x}_2\dot{x}_3 + \dot{x}_3\dot{x}_1 + \exp(2x_1) + \exp(x_2 - x_1) + \exp(x_3 - x_2), \quad (10)$$

with the constraint (6) turning into [9]

$$\mathcal{H} := \sum_{i=1}^3 \frac{\partial \mathcal{L}}{\partial \dot{x}_i} \dot{x}_i - \mathcal{L} = \dot{x}_1\dot{x}_2 + \dot{x}_2\dot{x}_3 + \dot{x}_3\dot{x}_1 - \exp(2x_1) - \exp(x_2 - x_1) - \exp(x_3 - x_2) = 0. \quad (11)$$

Equation (11) clarifies the sense of the dependence between (5) and (6): the constraint (6) is a particular choice of the first integral \mathcal{H} for solutions of equations (5), namely $\mathcal{H} = 0$.

The Lagrangian (10) has a well defined potential and kinetic “energies”. The latter is an indefinite quadratic form of signature $(+, -, -)$, whose zero surface is a cone. As seen from (11), the “potential energy” is always negative while the “total energy” is zero. This means that the “kinetic energy” is positive, i.e., position of the system in the space of “velocities” varies inside a cone (further on, the quotation marks will be omitted, also for the accelerations, i.e., derivatives of the velocities, as well as the kinetic, potential and total energies).

III. METHODS

We apply the aforementioned Lagrangian formalism, and illustrate the evolution of the system by its trajectory in the space of velocities in the diagonalized version of Lagrangian (10) (defined below, in the first subsection).

A. Useful variables

Transformation (9) naturally replaces the original variables a, b, c by their logarithms x_1, x_2, x_3 , suitable for the Lagrangian description. However, the description becomes clearer if we diagonalize the kinetic energy. If we care about simplicity of the equations rather than unitarity of the diagonalizing transformation (accepting its determinant to be -6), a convenient substitution is

$$x_1 = u_1 - u_2 - u_3, \quad x_2 = u_1 + 2u_3, \quad x_3 = u_1 + u_2 - u_3, \quad (12)$$

which yields the Lagrangian in the form diagonal in the velocities $\dot{u}_1, \dot{u}_2, \dot{u}_3$,

$$\mathcal{L} = 3\dot{u}_1^2 - \dot{u}_2^2 - 3\dot{u}_3^2 + \exp(2(u_1 - u_2 - u_3)) + \exp(u_2 - 3u_3) + \exp(u_2 + 3u_3). \quad (13)$$

Variables u_1, u_2, u_3 define the principal directions in the velocity space. The dynamics in the new variables is determined by the Lagrange equations

$$\ddot{u}_1 = \frac{1}{3}e^{2(u_1 - u_2 - u_3)}, \quad (14a)$$

$$\ddot{u}_2 = e^{2(u_1 - u_2 - u_3)} - e^{u_2} \cosh(3u_3), \quad (14b)$$

$$\ddot{u}_3 = \frac{1}{3}e^{2(u_1 - u_2 - u_3)} - e^{u_2} \sinh(3u_3). \quad (14c)$$

with the constraint

$$\mathcal{H} := 3\dot{u}_1^2 - \dot{u}_2^2 - 3\dot{u}_3^2 - e^{2(u_1 - u_2 - u_3)} - 2e^{u_2} \cosh(3u_3) = 0. \quad (14d)$$

In terms of the original variables, the new ones are

$$u_1 = \frac{1}{3} \ln(abc), \quad u_2 = \frac{1}{2} \ln(c/a), \quad u_3 = \frac{1}{6} \ln(b^2/ac). \quad (15)$$

As we can see, u_1 is the logarithm of the volume scale, up to a multiplicative constant. Hence, the diagonalization automatically separates dynamics of the volume from that of the shape, thus doing what Misner introduced in the first stage of his transformation for the Mixmaster model [5].

The velocities might simply be expressed in terms of the canonical momenta $p_i = \partial \mathcal{L} / \partial \dot{u}_i$, $i = 1, 2, 3$; then \mathcal{H} would become the Hamiltonian, whose kinetic part was also a diagonal quadratic form in the momenta. However, the momenta are equal to the velocities, up to a multiplicative constant. Therefore, we do not introduce extra momentum-variables.

Variables a, b, c are not suitable for numerical simulations, especially for their graphic presentation, because of the disproportion between their sizes $a \gg b \gg c$. This purpose is better served by quantities of equal order of magnitude. The shape of equations (5) and (6) suggest that these could be

$$q := a^2, \quad r := b/a, \quad s := c/b, \quad (16)$$

while their logarithmic counterparts

$$y_1 := \ln q, \quad y_2 := \ln r, \quad y_3 := \ln s, \quad (17)$$

allow for the corresponding Lagrangian description. A simple manipulation of the original equations (5) leads to those satisfied by the new variables, which may be cast into a compact form

$$\begin{pmatrix} \ln q \\ \ln r \\ \ln s \end{pmatrix}'' = M \cdot \begin{pmatrix} q \\ r \\ s \end{pmatrix}, \quad \text{or} \quad \begin{pmatrix} \ddot{y}_1 \\ \ddot{y}_2 \\ \ddot{y}_3 \end{pmatrix} = M \cdot \begin{pmatrix} e^{y_1} \\ e^{y_2} \\ e^{y_3} \end{pmatrix} \quad (18)$$

with the constraint given by

$$\frac{1}{2} (\ln q \ \ln r \ \ln s)' \cdot M^{-1} \cdot \begin{pmatrix} \ln q \\ \ln r \\ \ln s \end{pmatrix}' - q - r - s = 0 \quad (19)$$

where the constant matrix M is given by

$$M = \begin{pmatrix} -2 & 2 & 0 \\ 2 & -2 & 1 \\ 0 & 1 & -2 \end{pmatrix}, \quad \text{with} \quad \det M = 2, \quad M^{-1} = \begin{pmatrix} \frac{3}{2} & 2 & 1 \\ 2 & 2 & 1 \\ 1 & 1 & 0 \end{pmatrix}. \quad (20)$$

The simplicity of equations (18) is due to the fact that the r.h.s. of the BKL equations (5) are linear combinations of q, r and s from (16). This makes them convenient variables for description of the BKL scenario. Their version for y_i , $i = 1, 2, 3$ may be derived from a simple Lagrangian

$$\mathcal{L} = \frac{1}{2} (\dot{y}_1 \ \dot{y}_2 \ \dot{y}_3) \cdot M^{-1} \cdot \begin{pmatrix} \dot{y}_1 \\ \dot{y}_2 \\ \dot{y}_3 \end{pmatrix} + e^{y_1} + e^{y_2} + e^{y_3} \quad (21)$$

The constraint again corresponds to $\mathcal{H} = 0$, where \mathcal{H} differs from the Lagrangian (21), by the opposite signs at the exponential functions. Explicitly

$$\mathcal{H} = \frac{3}{4}\dot{y}_1^2 + 2\dot{y}_1\dot{y}_2 + \dot{y}_2^2 + \dot{y}_2\dot{y}_3 + \dot{y}_3\dot{y}_1 - (e^{y_1} + e^{y_2} + e^{y_3}) = 0. \quad (22)$$

Diagonalization of the kinetic energy in the Lagrangian (21), is achieved by substitution of y_1 , y_2 and y_3 with their values in terms of u_1 , u_2 and u_3 respectively

$$y_1 = 2(u_1 - u_2 - u_3), \quad y_2 = u_2 + 3u_3, \quad y_3 = u_2 - 3u_3, \quad (23)$$

which leads back to Lagrangian (13) and the constrained Lagrange equations which stem from it (14).

B. The cone of kinetic energy

Our basic geometric tool for analysis and presentation of the dynamics will be the quadrics of kinetic energy.

$$E_k := 3\dot{u}_1^2 - \dot{u}_2^2 - 3\dot{u}_3^2 = \epsilon \geq 0. \quad (24)$$

For $\epsilon > 0$ these are two-sheet hyperboloids, becoming a cone for $\epsilon = 0$.

Assume that the initial conditions describe a universe, whose volume is decreasing. In the variables \dot{u}_1 , \dot{u}_2 and \dot{u}_3 , we have

Proposition 1. *The dynamics of the universe which shrinks with τ takes place in the lower interior of the cone*

$$3\dot{u}_1^2 - \dot{u}_2^2 - 3\dot{u}_3^2 > 0, \quad \dot{u}_1 < 0. \quad (25)$$

Proof. The first inequality (*interior*) follows from the constraint (14d), from which $3\dot{u}_1^2 - \dot{u}_2^2 - 3\dot{u}_3^2$ is equal to a sum of exponential functions and hence it is positive. The second (*lower*, i.e. $\dot{u}_1 < 0$), is equivalent to the assumption that the volume scale is decreasing, by the first equation of (15). \square

The following properties make the cone of kinetic energy a particularly useful tool, reproducing essential information that phase diagrams provide for single functions:

Proposition 2. *Zero of the kinetic energy, i.e. the conical surface $3\dot{u}_1^2 - \dot{u}_2^2 - 3\dot{u}_3^2 = 0$ is a singular manifold of the solutions.*

Proof. From the constraint (14d), if the kinetic energy E_k turns to zero, then the sum of exponential functions (the minus potential energy, $-E_p$) also has to be zero, whence all exponents in (23) tend to $-\infty$ on approach to the surface (including its apex). This requires that at least u_1 and u_2 tend to $-\infty$. \square

Corollary. *Bearing in mind that the accelerations \ddot{u}_i , $i = 1, 2, 3$, are linear combinations of these exponential functions (see (14)), we see that all of them tend to 0, i.e., the rate of approach to the singular surface slows down to zero.*

Later, we will see that the trajectory of the system gets reflected from one of the hyperboloid surfaces (24) before attaining the singularity, with the exception of the exact solution (30). With this exception, the conical surface is never reached, even in the limit $\tau \rightarrow \infty$.

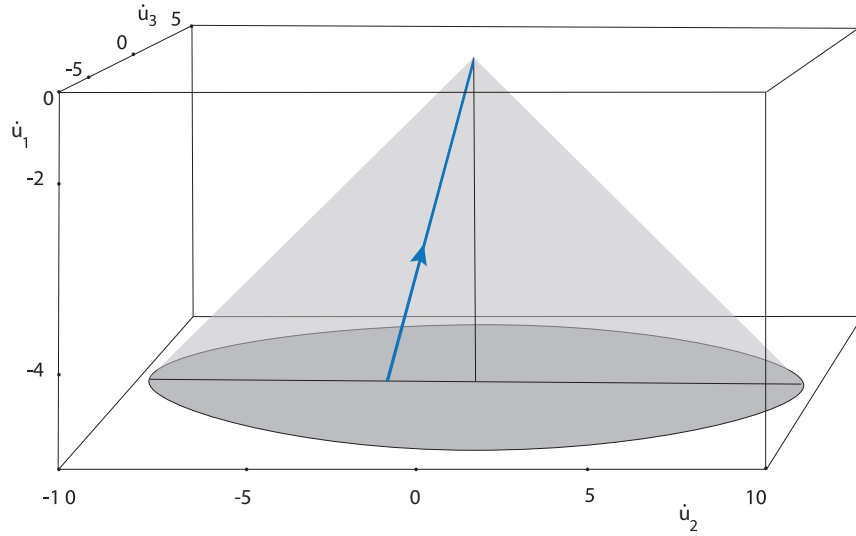


FIG. 1. (from [12]). The lower half (= universe shrinking with τ) of the cone $3\dot{u}_1^2 - \dot{u}_2^2 - 3\dot{u}_3^2 > 0$. The dynamics of the system takes place inside the cone. The line with the arrow shows the exact solution; the arrow indicates its direction of evolution. For $\tau \rightarrow \infty$, the line tends to the apex of the cone.

A position in the cone, together with the tangent to the trajectory, provide complete information on u_1, u_2, u_3 , and their derivatives.

Proposition 3. *The position of the system in the cone, together with the direction of the tangent to the trajectory, provide complete information on the local values of u_1, u_2, u_3 and their τ derivatives.*

Proof. The Cartesian coordinates of the position in the cone are the components of the velocity, \dot{u}_1, \dot{u}_2 and \dot{u}_3 . The direction of the tangent yields proportions between the components of the acceleration \ddot{u}_1, \ddot{u}_2 and \ddot{u}_3 . Given the components of the velocity, the length of the acceleration vector can be retrieved from

$$2\ddot{u}_2 - 9\ddot{u}_1 + 3\dot{u}_1^2 - \dot{u}_2^2 - 3\dot{u}_3^2 = 0, \quad (26)$$

which is a simple linear combination of equations (14a), (14b) and (14d) (the exceptional case which would not yield the length is $\ddot{u}_2/\ddot{u}_1 = 9/2$, but this might happen only on the conical surface). Having the accelerations, we can calculate the values of u_1, u_2 and u_3 by solving the system (14a), (14b), (14c) for these variables.

By differentiation of these equations, we can obtain higher derivatives of u_i , $i = 1, 2, 3$, if they exist. \square

Remark. *Consequently, this means that the aforementioned data uniquely determine the scale factors a, b and c and their derivatives (by inversion of (15)).*

Proposition 4. *Each of the velocities, \dot{u}_1 , \dot{u}_2 and \dot{u}_3 , has a finite limit as $\tau \rightarrow \infty$.*

Proof. A simple, reversible linear transformation turns the dynamics equations (14a), (14b), (14c), into

$$3\ddot{u}_1 = e^{2(u_1 - u_2 - u_3)}, \quad (27a)$$

$$4\ddot{u}_1 - \ddot{u}_2 - \ddot{u}_3 = e^{u_2 + 3u_3} \quad (27b)$$

$$2\ddot{u}_1 - \ddot{u}_2 + \ddot{u}_3 = e^{u_2 - 3u_3} \quad (27c)$$

The r.h.s. of the resulting equations are exponential functions and hence they are positive, whence their l.h.s. are second derivatives of convex functions and first derivatives, of increasing functions, \dot{u}_1 , $4\dot{u}_1 - \dot{u}_2 - \dot{u}_3$ and $2\dot{u}_1 - \dot{u}_2 + \dot{u}_3$, respectively. The latter functions are bounded, because the increasing property of \dot{u}_1 , together with $\dot{u}_1(0) < 0$, infer $|\dot{u}_1(t)| < |\dot{u}_1(0)|$, while both $|\dot{u}_2(t)|$ and $|\dot{u}_3(t)|$ are not greater than $\sqrt{3}|\dot{u}_1(t)|$ as long as we are inside the cone. Hence, all three linear combinations of the first derivatives are increasing functions bounded from above, and thus have finite limits.

The limits $g_1 := \lim_{\tau \rightarrow \infty} \dot{u}_1$, $g_2 := \lim_{\tau \rightarrow \infty} \dot{u}_2$ and $g_3 := \lim_{\tau \rightarrow \infty} \dot{u}_3$ may be uniquely regained from the limits of these linear combinations by inverting the transformation which leads from (14) to (27). \square

Corollary. *As \dot{y}_i , $i = 1, 2, 3$, are linear combinations of \dot{u}_i (23), they also have finite limits. Moreover, as the corresponding linear transformation is nonsingular, all \dot{y}_i vanish at the apex and only at the apex. Also, for all i , $y_i \rightarrow -\infty$ for $\tau \rightarrow \infty$, which is a consequence of the constraint (22).*

Proposition 5. *A trajectory which ends on the surface or at the apex of the cone, needs infinite time τ to reach it.*

Proof. Consider a trajectory beginning in the lower half of the cone and ending on its surface or apex. Since, $\dot{u}_1 < 0$, hence u_1 is a decreasing function of τ . On this basis, τ may be calculated as

$$\tau = \int_{u_1(0)}^{u_1} du'_1 / \dot{u}'_1 \quad (28)$$

From (14a) and (25), we have $0 > \dot{u}_1(t) \geq \dot{u}_1(0)$ in the lower interior of the cone, whence $1/\dot{u}_1(t) \leq 1/\dot{u}_1(0) < 0$. Hence the integrand $1/\dot{u}'_1$ is separated from 0 in the interval of integration. On the other hand, $u_1 \rightarrow -\infty$ when we approach the boundary (see the proof of Proposition 2). The integral (28) in the limit $u_1 \rightarrow -\infty$ extends over infinite interval, while its integrand is separated from zero. Hence, it is infinite. \square

Remark. *The time parameter τ calculated in (28), over a finite or infinite interval, is always positive, because the integrand is negative, while the lower limit of integration is greater than the upper limit.*

Proposition 6. (converse of Proposition 5)

In the limit $\tau \rightarrow \infty$, each trajectory reaches the surface or apex of the cone.

Proof. Time τ can also be expressed as

$$\tau = \int_{\dot{u}_1(0)}^{\dot{u}_1} d\dot{u}'_1 / \ddot{u}'_1, \quad (29)$$

because \dot{u}_1 is an increasing function of τ due to the positive sign of its derivative (14a). For any point of the lower interior of the cone, the denominator is greater than zero (from (14a)), whence the integrand is finite and so are the limits of integration. Hence τ has a finite value. Merely for $(\dot{u}_1, \dot{u}_2, \dot{u}_3)$ lying on the surface or at the apex of the cone can \ddot{u}_1 vanish and τ become infinite. \square

Corollary. *This means that points on a trajectory in the interior of the cone are attained in a finite time.*

Remark. *Variable \dot{u}_1 (which is the logarithmic derivative of the volume scale) might in principle replace time parameter τ , as it is an increasing function of τ . Nevertheless, its use for this purpose is limited, as its variation is very uneven (see Fig. 2). There are intervals of τ where the exponential function in (14a) is close to zero and thus \dot{u}_1 hardly increases. This happens at each approach to the conical surface, (i.e. when the kinetic energy decreases to nearly 0). Then also the other exponential components in (14) become very small (see Fig. 2, 3). We discuss this Kasner-type behavior in subsection VIB.*

Proposition 7. *Trajectories in the interior of the cone contain nonsingular, nonzero points of solutions to (5), (6).*

Proof. Consider points in the interior of the cone, lying on a trajectory of a solution in the \dot{u}_i space, $i = 1, 2, 3$. The coordinates u_i are finite as integrals of finite \dot{u}_i over a finite τ interval. Hence y_i are also finite as linear combinations of the respective u_i , whence a^2 , b/a and c/a are finite and positive as they are equal to $\exp y_1$, $\exp y_2$ and $\exp y_3$ respectively (see (17)). This guarantees that also the scale factors a , b and c are finite and nonzero. \square

Finally,

Proposition 8. *There is no possibility of a stop in the interior of the cone (i.e., each point of positive kinetic energy corresponds to nonzero acceleration).*

Proof. This property follows directly from equation (26). As long as $3\dot{u}_1^2 - \dot{u}_2^2 - 3\dot{u}_3^2 > 0$, we have $2\ddot{u}_2 - 9\ddot{u}_1 < 0$, which requires at least one nonzero component of the acceleration. \square

Situations where the trajectory in the velocity space slows down to almost full stop may happen (see Fig. 2), which corresponds to the Kasner-type behavior discussed in subsection VIB.

IV. SOLUTIONS ENDING AT THE APEX OF THE CONE

A. The exact solution in the cone

In terms of the u_i variables, the exact solution reads

$$u_1 = \frac{1}{3} \ln \frac{10800}{|\tau - \tau_0|^9}, \quad u_2 = \frac{1}{2} \ln \frac{40}{|\tau - \tau_0|^4}, \quad u_3 = \frac{1}{6} \ln \frac{5}{2}. \quad (30)$$

Obviously, for $\tau > \tau_0$, both \dot{u}_1 and \dot{u}_2 are proportional to $(\tau - \tau_0)^{-1}$, while $\dot{u}_3 = 0$. We also have $\dot{u}_2 = \frac{2}{3}\dot{u}_1$, which means that the trajectory corresponding to the exact solution is a half-line whose end lies at the apex of the cone (see Fig. 1). Physically, it describes a

power-like collapse of all scale factors a, b, c to zero, i.e. a collapse of the universe, in all directions, to a point, as $\tau \rightarrow \infty$ (which corresponds to the original time tending to zero from the right).

The instability of the exact solution, found in [12] affects also the solution in terms of u_i , only the coefficients at the oscillatory terms are different. However, the solution itself is regular up to the apex.

B. On the uniqueness of the exact solution

Due to the assumed indefinitely growing anisotropy, the ratios of the scale factors, a, b, c , always tend to 0 or ∞ for $\tau \rightarrow \infty$. Therefore, the limits of their proportions at $\tau \rightarrow \infty$ do not distinguish between various solutions. If we want to see the differences between their asymptotics, we have to raise them to appropriate powers to compensate for the anisotropy. E.g., if a is left at power 1, we have to raise $b^{1/3}$ and $c^{1/5}$ according to the Lie symmetry (8) (this can also be seen in the exact solution (7), where $b/a^3 = 10/9$, while $c/a^5 = 40/81$).

Hence the question from the title of the subsection may be formulated as: “is the all-direction collapse possible with any other proportion of the scale factors at appropriate powers?”.

Instead of proportion between these powers of b, c and a , we may use their 1 : 1 counterparts in the proportions between q, r, s (defined in (16)), without this somewhat artificial raising to powers. This is possible thanks to

$$b/a^3 = r/q, \quad c/a^5 = (r/q)(s/q). \quad (31)$$

This way, if finite or infinite limits of the l.h.s.’s of (31), exist, then also the ratios r/q and s/q have well defined limits, and vice versa. Therefore, we may consider the limits of the latter. Further, if they exist, then we have also well defined limits of their logarithms $y_2 - y_1$ and $y_3 - y_1$ respectively. By linear transformation (23) and the de l’Hôpital rule, we can also interpret this fact in our conical picture. Namely, this means that trajectories exist which approach the apex in a definite direction as $\tau \rightarrow \infty$.

The answer to the question of uniqueness is positive. Namely

Proposition 9. *The only asymptotic of solutions to equations (18), (19), which ensures existence of limits of $\lim_{\tau \rightarrow \infty}(r/q)$ and $\lim_{\tau \rightarrow \infty}(s/q)$ is that of the exact solution, i.e.*

$$q = \frac{9}{(\tau - \tau_0)^2}, \quad r = \frac{10}{(\tau - \tau_0)^2}, \quad s = \frac{4}{(\tau - \tau_0)^2}, \quad (32)$$

which is equivalent to (7) upon substitution (16).

The proof has been put off to Appendix A.

Remark. *Existence of the above limits means (by de l’Hôpital’s rule) that also the corresponding limits $\lim_{\tau \rightarrow \infty} \dot{r}/\dot{q}$ and $\lim_{\tau \rightarrow \infty} \dot{s}/\dot{q}$ exist, because the constraint (19) requires that $q \rightarrow 0, r \rightarrow 0, s \rightarrow 0$ whenever the kinetic term vanishes, i.e. for any y_1, y_2, y_3 on the conical surface or at the apex.*

V. SOLUTIONS APPROACHING THE LATERAL SURFACE OF THE CONE

From Proposition 6, we know that the trajectory has to approach the apex (as the exact solution) or the lateral surface of the cone. In this section, we discuss the latter case.

A. Asymptotics of the diagonal velocities

Let a trajectory approach the conical surface, but not the apex. According to Proposition 4, all three velocities have their limits at $\tau \rightarrow \infty$, namely $\dot{u}_i \rightarrow g_i$, $i = 1, 2, 3$, $g_1 \neq 0$. If the limits were on the surface, they would satisfy the equation of the cone

$$3g_1^2 - g_2^2 - 3g_3^2 = 0 \quad (33)$$

With $\dot{u}_i \rightarrow g_i$, the asymptotic behavior of the diagonal variables is $u_i \sim g_i \tau$. Translating dependence between u_i and a, b, c (15) into the corresponding asymptotics of the scale factors, according to (15), we obtain

$$a \sim \exp(p_1 \tau), \quad b \sim \exp(p_2 \tau), \quad c \sim \exp(p_3 \tau) \quad (34)$$

where $p_1 = g_1 - g_2 - g_3$, $p_2 = g_1 + 2g_3$, $p_3 = g_1 + g_2 - g_3$.

We could put any common coefficient in front of p_i , $i = 1, 2, 3$ by changing the scale of the time parameter τ (this was done in [6]). By straightforward calculation, equation (33) turns into a constraint on the constants p_i

$$p_1 p_2 + p_2 p_3 + p_3 p_1 = 0, \quad (35)$$

which by rescaling of τ (including its direction) so that $p_1 + p_2 + p_3 = 1$ (first Kasner's condition (2) [5]) is equivalent to the second Kasner's condition (2), in accordance with [6]. This result means that if a trajectory of a solution ended on the conical surface, it would describe an exact Kasner's solution: the universe would be squeezed to zero in one direction while being stretched to infinity in the remaining two. Conversely, if p_i satisfy the Kasner conditions (2), then the corresponding point (g_1, g_2, g_3) lies on the surface of the cone.

B. Impossibility of the exact Kasner asymptotics

Numerical calculation (see Fig. 3) shows that the Kasner solutions are reproduced with high precision by solutions of the BKL. However, the aforementioned exact Kasner-type solutions, though predicted and described in [6], do not exactly satisfy the BKL equations (5), (6) (which is acceptable as these equations are approximate). In terms of the cone of kinetic energy, even in the limit $\tau \rightarrow \infty$ does not the trajectory of the system reach the lateral conical surface $E_k = 0$, $u_1 < 0$. Namely, it gets reflected from a hyperboloid $E_k = \epsilon > 0$ before reaching the boundary of the cone, although the minimum ϵ of the kinetic energy may be very small (see Fig. 3). This property means that

Proposition 10. *The only possible asymptotic behavior of solutions to (18), which satisfies constraint (22), corresponds to $\gamma_1 = \gamma_2 = \gamma_3 = 0$, where $\gamma_i = \lim_{\tau \rightarrow \infty} y_i$, $i = 1, 2, 3$.*

Remark. *This means that all solutions eventually end at the apex, i.e., the fate of the universe is a total collapse to a point (with the original time – if we follow the history of the universe backwards, we end at a point). According to Proposition 5, this happens only in the limit $\tau \rightarrow \infty$. Moreover, together with Proposition 9, it means that the collapse is always chaotic.*

The proof is lengthy and therefore it has been put off to Appendix B.

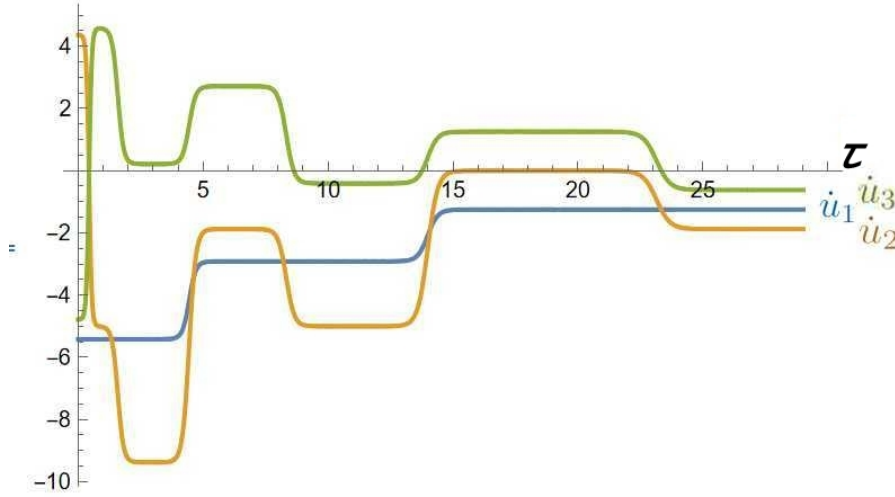


FIG. 2. Three components of the velocity, \dot{u}_1 , \dot{u}_2 and \dot{u}_3 , as functions of the time parameter τ . The initial conditions correspond to $q(0) = 0.225$, $r(0) = 0.25$, $s(0) = 0.1$, $\dot{q}(0) = -2, 25$, $\dot{r}(0) = -2, 5$. Each of the velocity components has time intervals of apparently constant value. Revealing their variability requires a logarithmic scale, as seen in the next figures.

VI. QUASI-KASNER SOLUTIONS

A. Description

Although exact Kasner solutions do not satisfy the system (5),(6), numerical calculations show that approximate Kasner-type solutions of these equations are possible and precise. Namely, the trajectories may approach the surface of the cone and bounce at a short distance from it, thus switching the universe to what may be considered the next Kasner epoch. The trajectory then passes through the interior of the cone until it approaches another point almost on its surface, at a less negative value of \dot{u}_1 (as this coordinate may only increase, according to (27a)). As the cone narrows, the amplitude of this quasi-periodic oscillations diminishes. This behavior corresponds to reflections from the potential walls on Misner's diagrams [5], while the surfaces of the corresponding quadrics (lower halves of the two-sheet hyperboloids)

$$3\dot{u}_1^2 - \dot{u}_2^2 - 3\dot{u}_3^2 = \epsilon_n \quad (36)$$

play the role of the equipotentials. The index n numbers the reflections while ϵ_n is a measure of its closeness to the surface of the cone.

Since the volume scale is proportional to $\exp(\frac{3}{2}u_1)$, while the time derivative, \dot{u}_1 , is negative throughout the evolution, the universe becomes more compact at subsequent reflections, although the reduction need not concern the scales in all directions.

Apparently, as seen in Fig. 2, the velocity components \dot{u}_i seem to remain constant for some time and the kinetic energy looks as if it were equal to zero in Fig. 3. A logarithmic scale is necessary to reveal the actual variation of these quantities in that figure. This is due to the exponential dependence of the derivatives on the values of these variables.

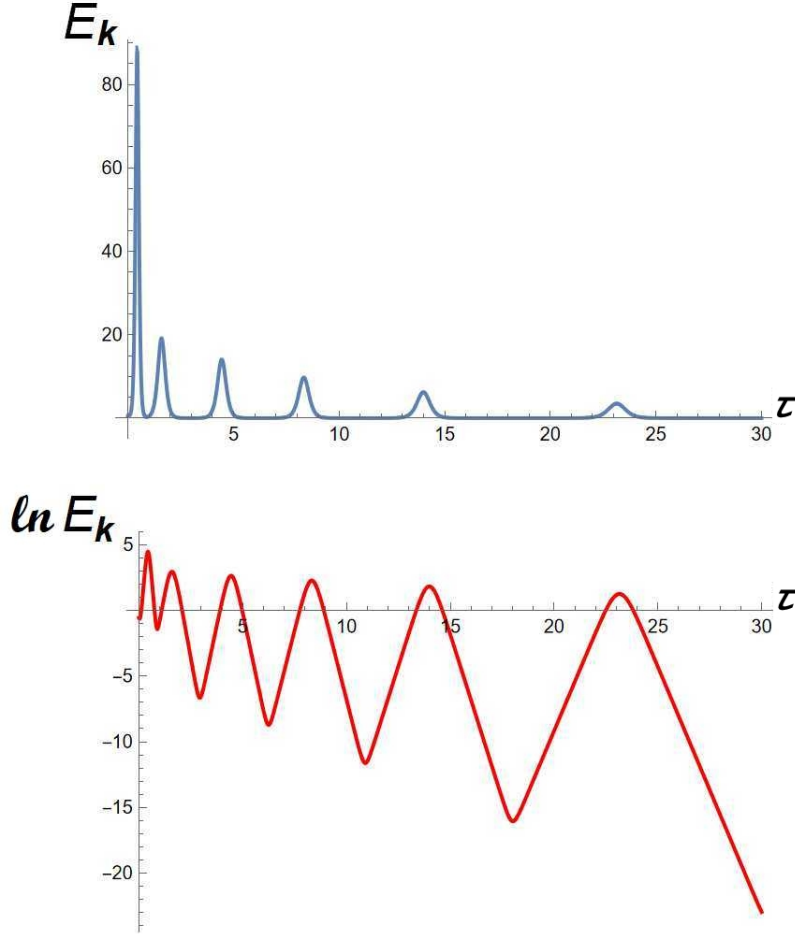


FIG. 3. The kinetic energy as a function of the time parameter τ for $q(0) = 0.225$, $r(0) = 0.25$, $s(0) = 0.1$, $\dot{q}(0) = -2, 25$, $\dot{r}(0) = -2, 5$. In the upper graph, apparently, E_k systematically reaches zero corresponding to the surface of the cone, and stays at this level for a long time, but the logarithmic scale in the lower graph reveals its sawtooth oscillations, with the teeth a little rounded (of shape $\ln \text{sech}^2$) at the reflections from the hyperboloidal surfaces (36).

B. Between Kasner's epochs

In [6], the consecutive switching between Kasner's epochs was extended from its original Mixmaster universe to the BKL scenario. This was achieved by assuming the l.h.s.'s of equations (5) to be zero, which was justified as an approximation of (5), (6) for large τ and slow variation. The solution was obtained in the form [6]

$$a = A_a \exp(2\Lambda p_a t), \quad b = A_b \exp(2\Lambda p_b t), \quad c = A_c \exp(2\Lambda p_c t), \quad (37)$$

where p_a , p_b and p_c satisfied the Kasner conditions (2). The authors noticed that the exponential dependence of the scale factors caused growing of the r.h.s. in equations (5) so that the approximation was no more valid after some time (or rather some τ). They stated that

this led to the exchange of the role of two scale factors, i.e. transition to the next Kasner epoch.

In this section, we examine this transition in more detail. The best variables for this purpose are the exponents y_1, y_2, y_3 and the corresponding exponential functions q, r, s , satisfying equations (18) and (19).

Let the trajectory described by the trio $(\dot{y}_1, \dot{y}_2, \dot{y}_3)$ closely approach a point $\gamma_1, \gamma_2, \gamma_3$ on the lateral surface of the cone. Without touching it, the trajectory would “bounce” from a potential wall according to (36) close to this point. Let $\tau = 0$ be the moment when the bounce occurs. Then the asymptotics of y_i , $i = 1, 2, 3$ would be

$$y_i^0 + \gamma_i \tau, \quad i = 1, 2, 3, \quad (38)$$

where y_i^0 are constants. In the generic case, all γ_i would be different. Hence, as τ increases, one of the exponents would soon become significantly larger than the two others; this would make one of the exponential functions $q = \exp y_1, r = \exp y_2, s = \exp y_3$ much greater than the remaining two. This disproportion of sizes allows for a reduction of (18) by retaining the largest of them in (18) while approximating the other two by 0 in some neighborhood of the turning point. The present approximation goes one step beyond the approximation of [6], which neglected all exponential functions, and thus it yields more information on the transition period. Note that the kinetic energy is equal to minus potential energy, $E_k = q + r + s$ (according to (19)). In the above approximation it reduces to only one term: the greatest of these three variables.

Whichever of the y_i is the greatest, we obtain an easily solvable system of ODE. If the dominant exponent is y_1 (for example), then the solution, with physically acceptable signs of the integration constants, after a short time from the turning, reads

$$q := a^2 = k_q^2 \operatorname{sech}^2 k_q(\tau - \tau_+), \quad (39a)$$

$$r := b/a = k_r^2 e^{\beta\tau} \cosh^2 k_q(\tau - \tau_+), \quad (39b)$$

$$s := c/b = k_s^2 e^{\gamma\tau}, \quad (39c)$$

where $\tau_+, k_q, k_r, k_s, \beta$ and γ are real constants, of which $\tau_+ > 0$, while k_q, k_r and k_s may be assumed positive. Consistency requires that $q \gg r$ and $q \gg s$ in some neighborhood of $\tau = \tau_+$. Hence $k_q \gg k_r$ and $k_q \gg k_s$. This ordering complies with the neglect of $r = \exp y_2$ and $s = \exp(y_3)$ in (39).

The constraint (19) limits the possible constant parameters; it requires $k_q^2 = \beta(\beta + \gamma)$, without any condition imposed on the other parameters.

At the turning point, an exchange of the dominant exponents should take place in the Kasner-type solutions. Indeed on the other side of the turning point the dominant term should be y_2 or y_3 , as y_1 decreases with the distance from τ_+ (and so does q), while at least one of y_2 (and r) or y_3 (and s) increases. It depends on the values of β and γ which of these would overcome y_1 (and q) at some distance from τ_+ . Consider, e.g. a transition from the situation where y_2 is the greatest of y_i for a little negative τ ; after the bounce at $\tau = 0$, y_1 becomes the greatest. Then, in some interval to the left of $\tau = 0$, we would have $r \gg q$ and $r \gg s$. The solution for these a little negative τ would read

$$q = k_q'^2 e^{\alpha\tau} \cosh^2 k_q'(\tau - \tau_-), \quad (40a)$$

$$r = k_r'^2 \operatorname{sech}^2 k_q'(\tau - \tau_-), \quad (40b)$$

$$s = k_s'^2 e^{\gamma_1\tau} \cosh k_q'(\tau - \tau_-), \quad (40c)$$

where the integration constants in (40), $\alpha, \tau_- < 0$, as well as positive k'_q, k'_r, k'_s , correspond to their counterparts for $\tau > 0$ in (39). Solutions (39) with (40) provide detailed picture of the dynamics in the right and left neighborhoods of the turning point $\tau = 0$. With the τ -distance from the turning point, the solutions containing the cosh and sech functions very soon turn into their asymptotics due to the rapid decay of their exp components having negative exponent, compared to those with the positive one. As a consequence, the asymptotics of their logarithms $y_1 = \ln q$, $y_2 = \ln r$ and $y_3 = \ln s$ are piecewise linear functions, e.g.

$$y_1 = \ln(4k_q^2) - 2k_q|\tau - \tau_+|, \quad y_2 = \ln(k_r^2/4) + \beta\tau + 2k_q|\tau - \tau_+| \quad (41)$$

on the positive side of $\tau = 0$, and

$$y_1 = \ln(k'_q{}^2/4) + \alpha\tau + 2k'_r|\tau - \tau_-|, \quad y_2 = \ln(4k'_r{}^2) - 2k'_r|\tau - \tau_-| \quad (42)$$

on the negative side. This way, each of these logarithmic variables undergoes a sawtooth oscillation (the tooth is blunt as the actual functions are logarithms of hyperbolic sech and cosh rather than the absolute values of $\tau - \tau_+$ and $\tau - \tau_-$). The linearity in the neighborhood of $\tau = 0$ is consistent with the assumed equations (38), provided that we adjust the parameters of the lines, namely, they must satisfy

$$\begin{aligned} k_q &= \frac{\gamma_1}{2}, \quad k'_r = -\frac{\gamma_2}{2}, \quad k'_q = \frac{2}{|\gamma_1|} \exp \frac{y_1^0 + y_2^0}{2}, \quad k_r = \frac{2}{|\gamma_2|} \exp \frac{y_1^0 + y_2^0}{2} \\ \alpha &= \beta = \gamma_1 + \gamma_2, \quad \tau_+ = (\ln \gamma_1^2 - y_1^0) / \gamma_1, \quad \tau_- = (\ln \gamma_2^2 - y_2^0) / \gamma_2. \end{aligned} \quad (43)$$

This way, the position (γ_1, γ_2) of the bounce, together with the values y_1^0 and y_2^0 completely determine the local evolution. Together with the y_3 data we would have 6 parameters, reduced to 5 by the constraint (22), which turns into $\gamma_3 = -(\frac{3}{4}\gamma_1^2 + 2\gamma_1\gamma_2 + \gamma_2^2) / (\gamma_1 + \gamma_2)$.

Equation (41) describes also the behavior of $\ln E_k$, as the contributions of r and s to E_k are negligible in the right neighborhood of $\tau = 0$, while the contributions of q and s may be neglected in its left neighborhood. The result is sawtooth shape of the dependence $E_k(\tau)$, see Fig. 3. In the graph of q, r, s (Fig. 4), the kinetic energy would approximately be their upper envelope, as $E_k \approx \max(q, r, s)$.

For larger τ -distances from τ_+ , if only $k_q > -\beta$, i.e., $\gamma_1 > -\frac{2}{3}\gamma_2$, then the increasing function r of (39) grows fast with τ until it overtakes the decreasing function q , while the growth of s remains slow, if any (this depends on k_s). Thus y_1 is decreasing while y_2 is increasing. After some time τ , overtaking of y_1 by y_2 (and q by r) must happen. Later, the reciprocal situation would affect r . As long as $s \ll q$ and $s \ll r$, a sequence of exchanges between these two variables takes place (see Fig. 4). This way, we obtain sawtooth oscillations, alternating as in Fig. 4.

The above reversal of the ordering $q = a^2$ with $r = b/a$ is equivalent to reversing the order of a^3 and b , while the two are equal (up to a constant 9/10) for the exact solution. Similar situations (with the exact solution in the middle) occur for the other reversals.

If we wanted to follow the dynamics beyond the validity of the above approximation, we might take another step, considering the system (18), with only one of the exponential functions, $\exp y_1, \exp y_2, \exp y_3$ set to 0 in (18), while two of them remain nonzero. Such systems have been solved and discussed by Conte [14] as systems linked to the BKL scenario. These systems prove to be useful as approximations of the actual behavior in the scenario.

With the exception of case $b/a = r = \exp(y_2) \approx 0$, the solutions are much more complex than those for only a single nonzero $\exp(y_i)$. For this simplest case, the solution (mutatis

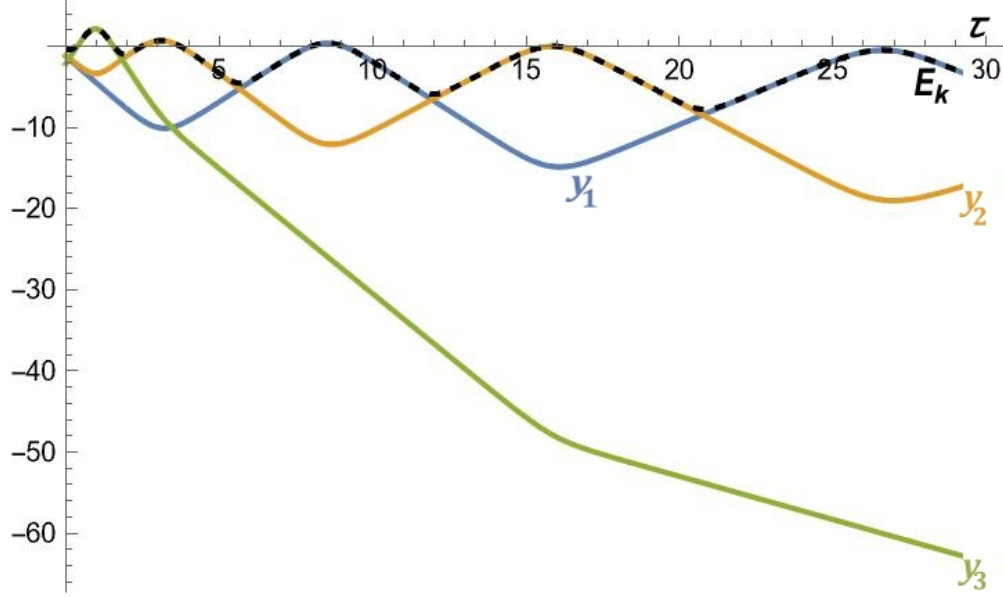


FIG. 4. The logarithmic variables $y_1 = \ln q$, $y_2 = \ln r$ and $y_3 = \ln s$ as functions of time parameter τ for $q(0) = 0.3$, $r(0) = 0.33$, $s(0) = 0.12$, $\dot{q}(0) = -1$, $\dot{r}(0) = -1$. Variables y_1 and y_2 exhibit sawtooth behavior, exchanging their dominant roles, while y_3 is much smaller. The kinetic energy E_k (dashed line) is the upper envelope of the y_i variables. The tips of the saw teeth are more rounded than those in the previous graph (Fig. 3) as the initial “velocities” are less than halves of those in Fig. 3. Still the term “sawtooth” is justified by the rectilinear shape of the teeth outside their blades.

mutandis equivalent to that of [14]) reads

$$q = k_q^2 \operatorname{sech}^2 k_q(\tau - \tau_-), \quad (44a)$$

$$r = k_r^2 e^{\alpha\tau} \cosh^2[k_q(\tau - \tau_-)] \cosh[k_s(\tau - \tau_3)], \quad (44b)$$

$$s = k_s^2 \operatorname{sech}^2[k_s(\tau - \tau_3)], \quad (44c)$$

where the constants τ_- and τ_3 are time values corresponding to the turning points of y_1 and y_3 respectively, while α , k_q , k_r and k_s have the similar sense as in the previous three cases. The kinetic energy is $q + s$, hence it is the sum of the two sech^2 functions.

In (44), it is evident, that also in this case the exchange takes place between the initially greater of q and s being surpassed by r , even though r was assumed to be 0 in the neighborhood of $\tau = \tau_+$. After this exchange, the solution (44) ceases to be valid.

The other two initial orderings which allow for approximating $s = 0$ or $q = 0$ on the r.h.s. of (18) lead to more refined solutions [14], namely to a solution expressed in terms of the Painlevé III function (for $s = 0$) or a more complex combination of exponential functions (for $q = 0$). As long as the neglected third component is actually unnecessary, as in Fig. 4, the Conte solutions precisely describe the actual behavior of the universe near the cosmological singularity within the BKL scenario.

VII. CONCLUSIONS

In the present work, the BKL scenario for the homogeneous universe in the neighborhood of the cosmological singularity is supplemented by a few exact results following from the BKL asymptotics of the Einstein equations. The Lagrangian-Hamiltonian version of the dynamics described by those equations is illustrated and analyzed by means of a simple geometric tool, a cone of the kinetic energy.

It was known that the approach to the singularity had oscillatory character [4, 6]. In this paper, a detailed description of the oscillations in the neighborhood of their turning points is derived as a solution to reduced equations. The oscillations are found to have sawtooth shape in the logarithmic variables and so is the shape of the logarithm of the kinetic energy. Solutions of other reduced equations, worked out in [14], may describe dynamics for a longer time, i.e., as long as one of the variables, a^2 , b/a , or c/b , remains significantly smaller than the other two as in Fig. 4. Whatever the oscillations be, the singularity relying on the collapse in all 3 dimensions must eventually happen in the limit $\tau \rightarrow \infty$ (i.e. $t \rightarrow 0^+$) for all initial (or final) conditions corresponding to decreasing volume $dV/d\tau|_{\tau=0} < 0$. Within the scenario, singularities of exact Kasner's shape do not happen, even in the limit $\tau \rightarrow \infty$. This means that never does the universe shrink to zero in some directions while extending to infinity in the others, like in the exact Kasner solutions (1), although the oscillations might approach such solutions closely. No singularity, of any type, may happen for finite τ . Finally, the exact solution derived in [12] is found to be the only one which describes the approach to the singularity with well-defined proportions between the directional scale factors (at the appropriate powers). Since [12] predicts instability of that exact solution, this means that the chaos on the approach to the singularity is inevitable.

Appendix A PROOF THAT ASYMPTOTIC OF THE EXACT SOLUTION IS THE ONLY PATH TO THE COLLAPSE WITH WELL-DEFINED PROPORTIONS BETWEEN q, r, s (PROPOSITION 9)

Proof. Plan: We will first (i) prove that all ratios y_i/y_j , $i, j = 1, 2, 3$, tend to 1. Then (ii) these limits yield the limits of ratios: $r/q \rightarrow 10/9$ and $s/q \rightarrow 4/9$, which are identical with the corresponding limits in the exact solution (32). Finally (iii), we find the asymptotic time dependence of q, r, s to be that of the exact solution, i.e., proportional to $(\tau - \tau_0)^{-2}$ with coefficients 9, 10, 4 respectively.

In these calculations we make use of de l'Hôpital's rule applied to quotients r/q and s/q (see Remark after Proposition 9) and to ratios y_i/y_j and \dot{y}_i/\dot{y}_j , $i, j = 1, 2, 3$. In particular, we have $\lim_{\tau \rightarrow \infty} y_i/y_j = \lim_{\tau \rightarrow \infty} \dot{y}_i/\dot{y}_j = \lim_{\tau \rightarrow \infty} \ddot{y}_i/\ddot{y}_j$, because for all i , $y_i \rightarrow -\infty$, while all $\dot{y}_i \rightarrow 0$, at the apex.

i) We have, from de l'Hôpital's rule

$$\lim_{\tau \rightarrow \infty} \frac{y_2}{y_1} = \lim_{\tau \rightarrow \infty} \frac{\ln r}{\ln q} = \lim_{\tau \rightarrow \infty} \frac{\dot{r}/r}{\dot{q}/q} = 1. \quad (45)$$

For other pairs chosen from y_1, y_2, y_3 and their respective counterparts q, r, s the procedure is identical.

ii) We may apply de l'Hôpital's rule twice, as the all-direction collapse means that the trajectory in the cone tends to the apex, whence $\dot{y}_i \rightarrow 0$ for all i . Using also the dynamics

equations (18) for replacement of the second derivatives of y_i , we obtain

$$1 = \lim_{\tau \rightarrow \infty} \frac{y_2}{y_1} = \lim_{\tau \rightarrow \infty} \frac{\ddot{y}_2}{\ddot{y}_1} = \lim_{\tau \rightarrow \infty} \frac{2(\exp y_1 - \exp y_2) + \exp y_3}{-2(\exp y_1 - \exp y_2)} = \lim_{\tau \rightarrow \infty} \frac{s}{2(r - q)} - 1, \quad (46)$$

where we have replaced $\exp y_i$ by the appropriate of q , r , or s . From (46), we get

$$\lim_{\tau \rightarrow \infty} s/(r - q) = 4 \quad (47)$$

By similar operations on y_3/y_1 , we obtain

$$1 = \lim_{\tau \rightarrow \infty} \frac{r - 2s}{2(r - q)}. \quad (48)$$

Substituting (47) to (48), we obtain

$$\lim_{\tau \rightarrow \infty} r/(r - q) = 10, \text{ whence } \lim_{\tau \rightarrow \infty} r/q = 10/9. \quad (49)$$

If the limit of $r/(r - q)$ is substituted from (49) to (47), we obtain

$$\lim_{\tau \rightarrow \infty} (s/r) = 4/10, \text{ whence } \lim_{\tau \rightarrow \infty} (s/q) = 4/9. \quad (50)$$

iii) The asymptotic τ dependence may be recovered from (26), which in terms of y_i has the form

$$\frac{3}{4}\dot{y}_1^2 + 2\dot{y}_1\dot{y}_2 + \dot{y}_2^2 + \dot{y}_1\dot{y}_3 + \dot{y}_2\dot{y}_3 - \frac{9}{2}\ddot{y}_1 - 5\ddot{y}_2 - 2\ddot{y}_3 = 0. \quad (51)$$

Dividing both sides of (51) by \dot{y}_1^2 and making use of the fact that all quotients \dot{y}_i/\dot{y}_1 and \ddot{y}_i/\ddot{y}_1 tend to 1, we obtain the asymptotic, which in the lowest order may be written as

$$\lim_{\tau \rightarrow \infty} \frac{d}{d\tau} \left(\frac{1}{\dot{y}_1} \right) = -\frac{1}{2}, \quad (52)$$

Integrating, we get the asymptotic of y_1 in the neighborhood of $\tau = \infty$

$$\dot{y}_1 = -2/(\tau - \tau_0), \quad y_1 = \ln \frac{C}{(\tau - \tau_0)^2}. \quad (53)$$

While the value of τ_0 is arbitrary, the value of C may be recovered by substitution of (53) into the constraint (22), which yields $C = 9$. Substitution of this C into (53) yields y_1 and $q = \exp y_1$ as in (32), then the asymptotics of r and s can be obtained from (49) and (50) respectively. This way, the asymptotic of any solution with well-defined limits of r/q and s/q proves to be identical with the exact solution (32), equivalent to (30) and (7) (for $\tau > \tau_0$). \square

Appendix B PROOF THAT ALL TRAJECTORIES EVENTUALLY TEND TO THE APEX (PROPOSITION 10)

We will prove it in two stages, using the y_i , $i = 1, 2, 3$ variables of (17) (which are connected with the scale factors by (16) and with the u_i through (23)).

Stage 1

Lemma. Let $\gamma_1, \gamma_2, \gamma_3$ be the limits of $\dot{y}_1, \dot{y}_2, \dot{y}_3$ (respectively) at $\tau \rightarrow \infty$. Then $\gamma_1 = \gamma_2 = 0$, while $\gamma_3 \leq 0$.

Proof. If for $\tau \rightarrow \infty$, the trajectory approaches the surface of the cone, then the kinetic part in the constraint (22) turns to zero. In terms of the limits γ_i

$$\frac{3}{4}\gamma_1^2 + 2\gamma_1\gamma_2 + \gamma_2^2 + \gamma_2\gamma_3 + \gamma_3\gamma_1 = 0 \quad (54)$$

The constraint (22) requires that the potential part also turns to 0. This means that the asymptotics $y_i = \gamma_i t + o(t)$, $i = 1, 2, 3$ has all $\gamma_i \leq 0$. To also satisfy (54), the first two of the γ_i 's must be equal to zero. \square

Stage 2: proof of Proposition 10

Proof. In the Lemma, we proved $\gamma_1 = \gamma_2 = 0$, $\gamma_3 \leq 0$. We are going to prove that $\gamma_3 < 0$ is impossible.

Assume $\gamma_3 < 0$. Adding first two equations in the right equation of (18), we obtain

$$\ddot{y}_1 + \ddot{y}_2 = \exp y_3. \quad (55)$$

Since $\lim_{\tau \rightarrow \infty} \dot{y}_3 = \gamma_3 < 0$, then for all $\varepsilon > 0$ a time parameter T exists such that for all $\tau > T$, we have

$$\dot{y}_3 \in]\gamma_3 - \varepsilon, \gamma_3 + \varepsilon[, \text{ whence } y_3 - y_3(T) \in](\gamma_3 - \varepsilon)(\tau - T), (\gamma_3 + \varepsilon)(\tau - T)[. \quad (56)$$

Choose ε such that $\gamma_3 + \varepsilon < 0$. We have, from (55),

$$\ddot{y}_1 + \ddot{y}_2 \in]e^{y_3(T) + (\gamma_3 - \varepsilon)(\tau - T)}, e^{y_3(T) + (\gamma_3 + \varepsilon)(\tau - T)}[, \quad (57)$$

with both exponents negative for sufficiently large τ . Hence, for these τ ,

$$\dot{y}_1 + \dot{y}_2 \in]\frac{1}{\gamma_3 - \varepsilon}e^{y_3(T) + (\gamma_3 - \varepsilon)(\tau - T)} + C_1, \frac{1}{\gamma_3 + \varepsilon}e^{y_3(T) + (\gamma_3 + \varepsilon)(\tau - T)} + C_1[, \quad (58)$$

where C_1 is a constant of integration. Since $\gamma_1 = \lim_{\tau \rightarrow \infty} \dot{y}_1 = 0$ and $\gamma_2 = \lim_{\tau \rightarrow \infty} \dot{y}_2 = 0$ (from the Lemma), we have $C_1 = 0$. Then, integrating again (58), we obtain

$$y_1 + y_2 \in]\frac{1}{(\gamma_3 - \varepsilon)^2}e^{y_3(T) + (\gamma_3 - \varepsilon)(\tau - T)} + C_2, \frac{1}{(\gamma_3 + \varepsilon)^2}e^{y_3(T) + (\gamma_3 + \varepsilon)(\tau - T)} + C_2[, \quad (59)$$

where C_2 is a constant of the next integration. However the constraint (22) requires that both $y_1 \rightarrow -\infty$ and $y_2 \rightarrow -\infty$ as $\tau \rightarrow \infty$, while both ends of the interval on the r.h.s. tend to a finite C_2 . Hence, the assumption $\gamma_3 < 0$ leads to a contradiction, whence $\gamma_3 = 0$.

The conclusion that all γ_i , $i = 1, 2, 3$ are equal to zero means that all trajectories tend to the apex. \square

[1] E. M. Lifshitz and I. M. Khalatnikov, "Investigations in relativistic cosmology", *Advances in Physics* **12**, Part 46, 185 (1963) <https://doi.org/10.1080/00018736300101283>

- [2] R. Penrose, “Gravitational collapse and space-time singularities” *Phys. Rev. Lett.* **14**, 57 (1965) <https://doi.org/10.1103/PhysRevLett.14.57>
- [3] S. W. Hawking, “Occurrence of singularities in open universes” *Phys. Rev. Lett.* **15**, 689 (1965) <https://doi.org/10.1103/PhysRevLett.15.689>.
- [4] V. A. Belinskii, I. M. Khalatnikov, and E. M. Lifshitz, “Oscillatory approach to a singular point in the relativistic cosmology”, *Adv. Phys.* **19**, 525 (1970) <https://doi.org/10.1080/00018737000101171>
- [5] Ch.W. Misner, K.S. Thorne and J.A. Wheeler, *Gravitation* (W.H. Freeman & Co., San Francisco 1973), §30.2 and §30.7
- [6] V. A. Belinskii, I. M. Khalatnikov, and M. P. Ryan, “The oscillatory regime near the singularity in Bianchi-type IX universes”, Preprint **469** (1971), Landau Institute for Theoretical Physics, Moscow; the part by V. A. Belinskii and I. M. Khalatnikov has been published as sections 1 and 2 in M. P. Ryan, *Ann. Phys.* **70**, 301 (1972) [https://doi.org/10.1016/0003-4916\(72\)90269-2](https://doi.org/10.1016/0003-4916(72)90269-2)
- [7] V. A. Belinskii, I. M. Khalatnikov, and E. M. Lifshitz, “A general solution of the Einstein equations with a time singularity”, *Adv. Phys.* **31**, 639 (1982) <https://doi.org/10.1080/00018738200101428>
- [8] V. A. Belinski, “On the cosmological singularity,” *Int. J. Mod. Phys. D* **23**, 1430016 (2014) <https://doi.org/10.1142/S021827181430016X>
- [9] E. Czuchry and W. Piechocki “Bianchi IX model: Reducing phase space” *Phys. Rev. D* **87**, 084021 (2013) <https://doi.org/10.1103/PhysRevD.87.084021>
- [10] E. Czuchry, N. Kwidzinski and W. Piechocki “Comparing the dynamics of diagonal and general Bianchi IX spacetime”, *Eur. Phys. J. C* **79**:173 (2019) <https://doi.org/10.1140/epjc/s10052-019-6690-y>
- [11] V. Belinski and M. Henneaux, “The Cosmological Singularity” (Cambridge University Press, Cambridge, 2017) <https://doi.org/10.1017/9781107239333>
- [12] P. Goldstein and W. Piechocki, “Generic instability of the dynamics underlying the Belinski-Khalatnikov-Lifshitz scenario” *Eur. Phys. J. C* **82**:216 (2022) <https://doi.org/10.1140/epjc/s10052-022-10158-7>
- [13] V. A. Belinskii and I. M. Khalatnikov, “On the nature of the singularities in the general solution of the gravitational equations”, *Sov. Phys. JETP* **29**, 911 (1969); translation from Russian of *Zh. Eksp. Teor. Fiz.* **56**, 1701 (1969)
- [14] R. Conte, “On a dynamical system linked to the BKL scenario”, *Phys. Scr.* **98** 105212 (2023) <https://doi.org/10.1088/1402-4896/acf4d3>
- [15] P.P. Goldstein “A Quadric of Kinetic Energy in the Role of Phase Diagrams – Application to the Belinski-Khalatnikov-Lifshitz Scenario”, *Geometric Methods in Physics XL Workshop Białowieża, Poland*, P. Kielanowski et al. eds. (Birkhäuser 2024), p. 331 <https://doi.org/10.1007/978-3-031-62407-0>